

# A DEM-CFD Approach for Predicting Pressure Drop through Packed Bed of Crushed Rocks

Elzubeir B.E. Hassan<sup>1</sup>[\[https://orcid.org/0000-0001-6869-8212\]](https://orcid.org/0000-0001-6869-8212) and  
J.E. Hoffmann<sup>2</sup>[\[https://orcid.org/0000-0002-5245-5061\]](https://orcid.org/0000-0002-5245-5061)

<sup>1, 2</sup> Stellenbosch University, South Africa

**Abstract.** Predicting the pressure drop over a packed bed of air-crushed rocks is a crucial parameter for a solar storage system to be economically viable. The selection of the blower and the estimation of the total capacity of the storage system are highly dependent on it. There are various parameters that influence the air flow through the bed, such as the shapes and sizes of the crushed rocks, which affect the packing density and particle arrangement. In this paper, the crushed rock was represented by an ellipsoidal shape with the same volume and aspect ratio as the average of randomly collected crushed rock samples to investigate the pressure drop through the packed bed. Simulation models were developed to assist in driving a pressure drop correlation as well as the effect of particles' orientation on pressure drop. For simulation, a Discrete Element Model (DEM) was used to generate the particles and Computational Fluid Dynamics (CFD) to simulate the flow over the particles. To validate the DEM/CFD models, experiments consisting of a packed bed of ellipsoidal particles and crushed rocks were developed. Consequently, an equation based on the porous media approach was proposed to predict the pressure drop, and the correlation was found to underestimate the pressure drop through the crushed rock by less than 20% in the horizontal flow.

**Keywords:** Thermal Energy Storage, Crushed Rocks, DEM/CFD Approach, Pressure Drop

## 1. Introduction

In the past two decades, renewable energy sources have been utilized to eliminate the harmful gas emissions that result from the combustion of fossil fuels. Solar energy is one of the renewable energy sources that has been widely utilized. This is because solar energy has the lowest operation cost and most abundant kind of energy, however its availability is limited by the sun's availability. To overcome this limitation, thermal energy storage (TES) systems have been proposed to store solar energy for night use. Typically, TES increases the overall efficiency of solar power plants, for example, by integrating the TES into a solarized Brayton/Rankine combined cycle. There are different types of materials that were utilized as storage mediums in the TES, including bricks, concrete, and rocks. To reduce the cost of the TES, the crushed rocks were the best choice among other packing materials. For instance, when crushed rocks are employed instead of two-tank molten salt, the cost of TES implementation can be decreased by one order of magnitude [1]. Furthermore, in order to minimize costs even further, a thorough understanding of the packed bed characteristics, particularly flow over rocks, is essential.

To accurately describe the flow behaviour through a crushed rock packed bed, the pressure drop must be accurately estimated, along with its correlations and influencing parameters. Therefore, several correlations for predicting the pressure drops in particle-packed beds have been developed. For one-dimensional flow, the pressure drop through a

packed bed of porous media (fixed bed) is typically calculated by adding two terms: the viscous component, which is proportional to velocity, and the inertial loss component, which is proportional to velocity squared [2]. Recent studies by Erdim et al., Allen et al., and Vollmari et al. [3] – [5] examined the most significant correlations used for spherical and non-spherical particles. However, all previous correlations are based on the semi-empirical Ergun equation [6]. The Ergun equation correlation is most employed in engineering practice to estimate the pressure drop across a packed bed of granular materials. Nevertheless, it cannot predict the pressure drop over an irregularly shaped bed with a Reynolds number greater than 1000 [5], [7] – [9].

Particle size and shape have a significant effect on the pressure drop. For that reason, several particle shapes have been proposed to represent crushed rocks, including bricks, connected spheres, and ellipses [10] – [12]. The ellipsoidal shapes were more effective at presenting the crushed rocks than the other shapes [13]. Hoffmann [12] examined the sizes of crushed rock by randomly measuring more than 100 particles and determined that the average box sizes are 87.9 mm, 59.5 mm, and 37.4 mm.

Due to the fact that it is impossible to predict the particles' motion in the CFD model, the DEM is used to export the particles to it [14]. For instance, Louw [11] utilized Nel's DEM model to develop his CFD model to simulate flow through non-spherical particles [15]. Also, Hoffmann and Lindeque [13] developed a CFD/DEM model to predict the pressure drop across a randomly packed bed of ellipsoidal particles. The model employed turbulent Reynolds number values and validated their results against an experimental model, resulting in viscous and inertial resistance tensors with constant values. However, they only looked at three orthogonal directions. In this publication, more investigation was done to estimate the pressure drop and the effect of particle orientation on it by examine more than 150 flow directions. The research is based on coupling DEM/CFD and a porous media technique for a packed bed of ellipsoidal particles.

## 2. Objectives and Methodology

The purpose of this work is to examine the effect of particle orientation on the flow characteristics and derive a pressure drop tensor across an anisotropic packed bed. As recommended by Hoffmann, the crushed rock was represented as an ellipsoidal to model the bed [12]. The ellipsoidal shape has the same volume and aspect ratio as the averages measured for roughly 100 rocks. To estimate the pressure drop, the packed bed was treated as a porous medium, and Equation 1 for momentum sink in CFD was used.

$$\mathbf{S}_i = \frac{\partial p}{\partial x_i} = - \left\{ \sum_{j=1}^3 \mathbf{D}_{ij} \mu + \sum_{j=1}^3 \mathbf{C}_{ij} \frac{1}{2} \rho |\vec{U}| \mathbf{u}_j \right\} \quad (1)$$

Where  $P$  is the pressure,  $\mu$  is fluid viscosity and,  $\rho$  the fluid density,  $\mathbf{u}_j$  the velocity components,  $|\vec{U}|$  the velocity magnitude, and  $\mathbf{D}_{ij}$ ,  $\mathbf{C}_{ij}$  are viscous and inertial resistance coefficients which depend on various factors including porosity ( $\epsilon$ ), particles' shape, size, roughness and orientation, fluid velocity and aspect ratio.

The average velocity through a packed bed of rock is approximately above 0.233 m/s [16]. Typically, as in Equation 1, the viscous factor is neglected as it is quite small in comparison with the inertial term. This is obviously shown in Figure 1, which displays the results for the Ergun correlation for both viscous and inertial terms, which are equal at 0.04m/s. Additionally, it is impossible to run the fan at a low speed during the validation stage, meaning that the pressure drop is too small to measure. Therefore, the equation can be rewritten as follows:

$$S_i = - \left\{ \sum_{j=1}^3 C_{ij} \frac{1}{2} \rho |\vec{U}| u_j \right\} \quad (2)$$

Equation 3 proposed by Einfeld and Schnitzlein for all types of fully developed flows was compared with Equation 2 to find an estimate pressure drop [17].

$$\frac{\Delta P}{L} = \frac{f \rho u^2 (1-\varepsilon)}{D_p \varepsilon^3} = f(Re_p) \quad (3)$$

Where  $D_p$  is the particle diameter or equivalent diameter for spherical particle and non-spherical shapes respectively, and  $f$  is the Darcy friction factor, which can be expressed as a function of particles' Reynolds number ( $Re_p$ ) as in the following equation [18]:

$$f = A Re_p^k \quad (4)$$

Where  $A$ , and  $k$  are constants.

Equation 2 can be rewritten as Equation 5 by substituting Equation 4 into Equation 3.

$$S_i = - \frac{2(1-\varepsilon)}{D_p \varepsilon^3} Re_p^k \sum_{j=1}^3 C_{ij} \frac{1}{2} \rho |\vec{U}| u_j \quad (5)$$

$$Re_p = \frac{\rho u D_p}{\mu (1-\varepsilon)} \quad (6)$$

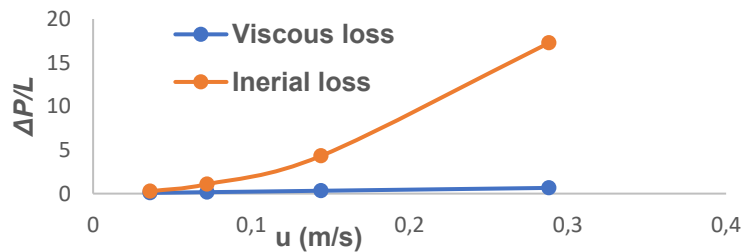


Figure 1. Relationship between viscous and inertial terms.

### 3. Numerical Models

The numerical model is composed of two stages. First, DEM is used to simulate particles packed randomly, and then CFD is used to simulate air flow through the bed.

#### 3.1 Discrete Element Modelling (DEM) Model

To allow for a fair comparison of the simulated and particle models, the DEM must first be calibrated using the angle of repose from a physical test. A shear stress box test was used to measure the angle of repose, utilizing multiple measurement methods. Figure 2a depicts the shear stress box, while Figure 2b depicts the various measurement techniques used. The angle of repose was 40.4 degrees, which was the average of the three measurement methods.

To calibrate the DEM to have the same angle of repose, numerous variables, including the static and dynamic frictions between particles and walls, were adjusted. The ellipsoidal particles were then poured into a spherical container with a diameter of 1,143 m along their

long axis (Y-direction), as shown in Figure 2c. Finally, the particles' information, including their position vector and orientation, were exported to a CSV file for use in SpaceClaim.

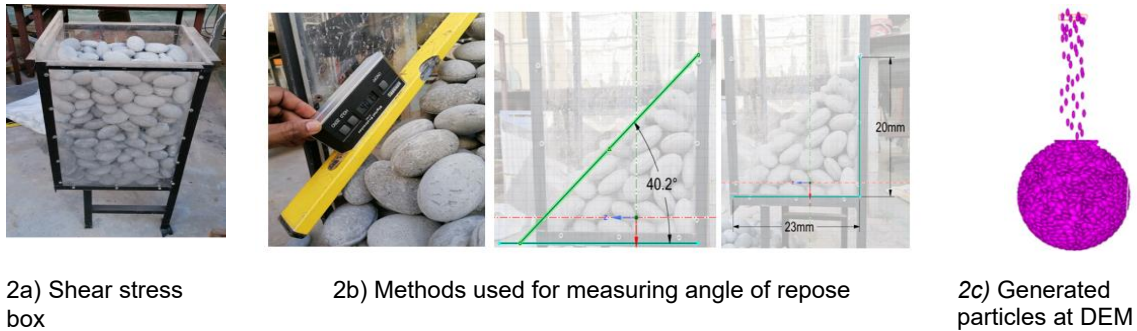


**Figure 2.** Method used for Rocky-DEM calibration and final DEM model.

### 3.2 CFD Model and Setup

The output from the DEM is utilized to generate SpaceClaim particles with the same local porosity. Using SpaceClaim, a master ellipsoidal particle was generated, which will serve as the standard for all subsequent particles. Using a Python script, the particles were given the same properties as the DEM-generated particles. The Python code uses the CSV file to rotate each ellipsoidal particle at the exact orientation and location as in Rocky-DEM. After that, the particles were subtracted from a cubic along the wind tunnel to reveal the flow domain, as shown in Figure 3. The flow was assumed to be horizontal with an angle of 0 degrees for elevation and azimuth. To investigate particle orientation, the angles of elevation and azimuth were varied from 0 to 180 degrees in increments of 15 degrees, resulting in 169 geometries.

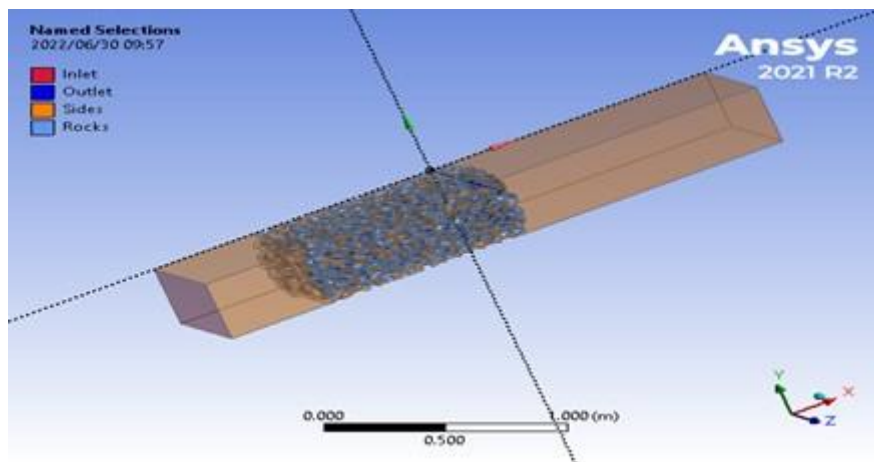


**Figure 3.** Geometry used into CFD.

The geometries were meshed using Fluent Mesher after the particles were shrunk by 2.25 percent to eliminate difficult-to-mesh contact regions. The poly-hexcore method was used to generate the volume mesh with a maximum of 5 mm cell sizes. This produced a mesh with an approximate volume mesh of 8 million cells. At the inlet of the wind tunnel, a constant velocity was maintained, and atmospheric pressure was set for the output. The K-epsilon model, a double pressure-velocity coupling system, and second-order upwind approaches were used in the configuration. After setting the residuals to  $10^{-6}$ , the simulation was run 5000 times, and a drop in pressure was recorded.

## 4. Experimental model

A packed bed of ellipsoidal particles model was developed experimentally to validate the CFD models. The ellipsoidal particles were cast using a 50/50 cement/sand mixture. They were then poured into the spherical cage formed from 10 mm steel bars and 1143 mm in diameter. The cage was constructed from 20 identical equilateral triangles joined by nuts and covered with a mesh sheet, as indicated in Figure 4. It was filled with 4,300 ellipsoidal particles weighing 0.210 kg each, for a total weight of approximately one ton that the overhead crane could lift. The bed porosity was computed using the total number of particles and the volume of the cage, assuming that the cage was spherical. To prevent leakage, the cage's sides were covered with Styrofoam, and the wooden box was sealed with masking tape at all joints.

As depicted in Figure 5, the experimental model was conducted in a wind tunnel at Stellenbosch University's Heat Transfer Laboratory. Five nozzles were used to regulate flow rate and inlet velocity in the wind tunnel. A variable-speed motor was also used to ensure that the air mass flow rate of the tested model was variable. The motor speeds and nozzles were utilized to alter the bed velocity. The pressure drop through an empty cage was initially measured, and after the bed was packed with particles, the pressure drop was also measured. As a consequence, the difference between the two pressure drop measurements can be used to calculate the pressure drop of the particle-filled bed.

The initial reading was taken in the horizontal plane at  $(0^\circ; 0^\circ)$  elevation and azimuth angles to serve as a reference for subsequent readings. The motor speed was altered to various speeds in order to generate various Reynolds numbers. To ensure the accuracy and validity of the measurements, the test was repeated multiple times for each motor speed. The final pressure drop measurement was estimated based on the average of multiple measurements. To examine the effect of particle alignment on the pressure drop through the packed bed, the cage was rotated by varying the elevation and azimuth angles from 0 to 180 degrees with a 15-degree anticlockwise increment. Finally, in order to obtain a different packing density, the cage was refilled with ellipsoidal particles and the testing procedure was repeated.



**Figure 4.** Casted ellipsoidal particles, spherical cage and filled model test.

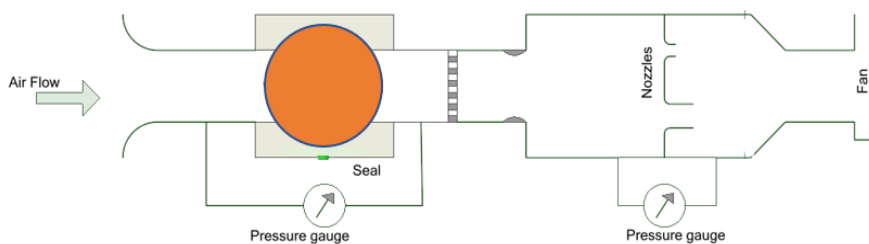


**Figure 5.** Wind tunnel general layout.

To validate the experimental test and CFD simulations of ellipsoidal particles, crushed rocks were implemented. The rocks were selected at random from the same pile of dolerite rocks that were used for size measurements done by Hoffmann [12], and the same procedure as previously described was applied.

## 5. Results and Discussion

In this section, the results from CFD of the ellipsoidal packed bed were compared with the experimental model. After that, both CFD and experimental models of the ellipsoidal particles were compared to crushed rocks. Figures 6 and 7 show the effects of azimuth and elevation angles on the pressure drop for both the CFD and the experimental models. It has been noticed that the change in pressure drop is mostly influenced by the variation of the elevation angle, with the greatest pressure drop occurring at 90 degrees. This implies the concept of the ellipsoidal shape lies along its long axis when allowing for free packing, as confirmed in Figure 8. It is worth mentioning that both models produced acceptable results and showed a high degree of similarity between them. However, small variations were discovered because of randomly packing the particles and it was calculated as a margin of error.

In Figure 6, the horizontal flow in both CFD and experimental models was obviously similar to the behaviour of crushed rocks. However, they both underestimated the reduction in pressure across the crushed rocks by about 20%. In Figure 7, the vertical flow, the measured pressure drop across the experimental model was about 10% less than the pressure across the crushed rocks. In contrast, the CFD model data overestimated the pressure drop across the crushed rocks by more than 40%. This is attributed to the fact that, in a vertical flow, DEM particles tend to lie on their long axis, which makes the bottom walls of the flow have a high coefficient of friction.

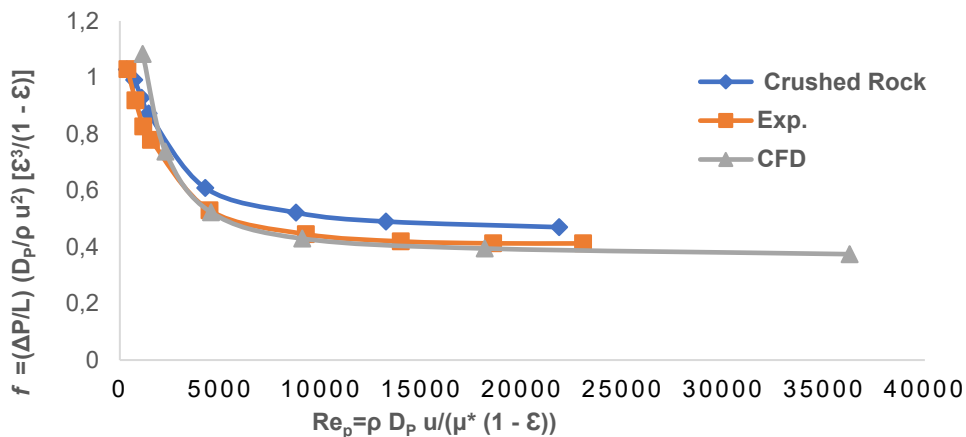


**Figure 6.** Horizontal flow for packed bed of ellipsoidal particles (CFD& experimental) and crushed rocks.

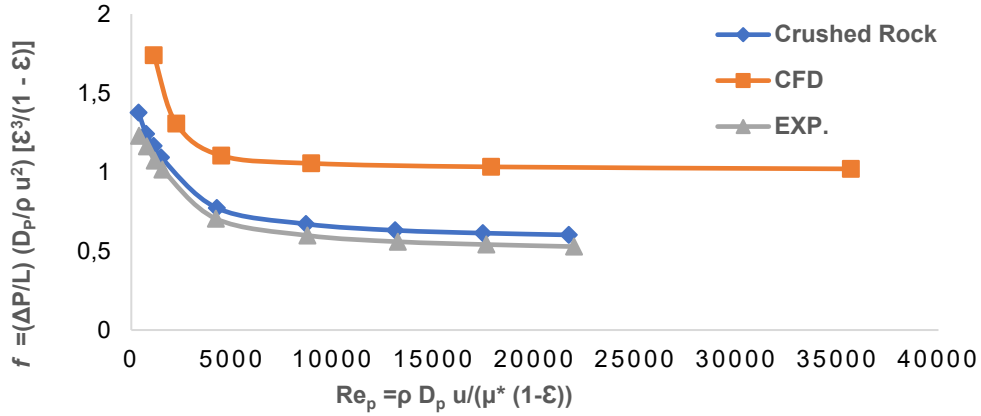


**Figure 7.** Vertical flow for packed bed of ellipsoidal particles (CFD& experimental) and crushed rocks.

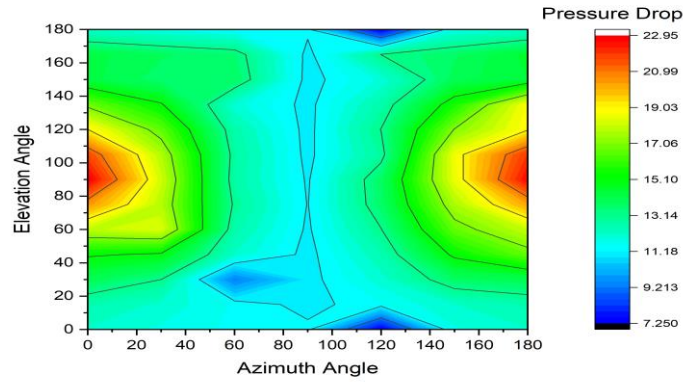


**Figure 8.** Effect of azimuth and elevation angles on the pressure drop at  $u=0.288$  m/s (CFD)

Figure 8 also demonstrates a high degree of symmetry between measurements of pressure drop. Typically, at the same elevation angles, the measurements at azimuth angles ranging from  $0^\circ$  to  $90^\circ$  (left side) were equivalent to those ranging from  $90^\circ$  to  $180^\circ$  (right side).

To develop a general correlation for the pressure, drop through a packed bed of rocks, the wall effect was excluded. The remaining particles depict crushed rock in an actual bed after a layer of three particles was removed. To drive the inertial tensors, the pressure drop through a packed bed of ellipsoidal particles was measured for 49 flow directions. The bed elevation and azimuthal angles relative to the global coordinate system were varied by  $15^\circ$  increments, and eight different velocities were used. The velocities began at 0.036 m/s and resulted in 392 measurement points. From each superficial velocity data point, a  $C_{ij}$  resistance tensor was computed, and then the mean tensor was derived. As depicted in Figure 9, the tensor elements were normalized by dividing them at their lowest velocity value, and then the power law to  $Re_p$  was computed (-0.242) with  $R^2 = 91\%$ . The computed standard deviation from the mean for diagonal and non-diagonal elements was less than 8%. Equation 7 is similar to that proposed by Hoffmann et al. [19], in which they stated that the power law of  $Re_p$  equal to (-0.227). Notably, the inertial resistance tensor was based on a skew-symmetric matrix with  $C_{ij} \approx C_{ji}$  and  $C_{ix} = -C_{iz}$ .

$$S_i = - \frac{2(1-\epsilon)}{D_p \epsilon^3} Re_p^{-0.242} \sum_{j=1}^3 C_{ij} \frac{1}{2} \rho |\vec{U}| u_j \quad (7)$$

$$C_{ij} = \begin{bmatrix} 17.64 \pm 0.89 & 28.44 \pm 0.60 & -17.46 \pm 0.89 \\ 33.92 \pm 2.86 & 55.25 \pm 1.93 & -33.92 \pm 2.86 \\ -15.47 \pm 0.37 & -25.20 \pm 0.25 & 15.47 \pm 0.37 \end{bmatrix}$$

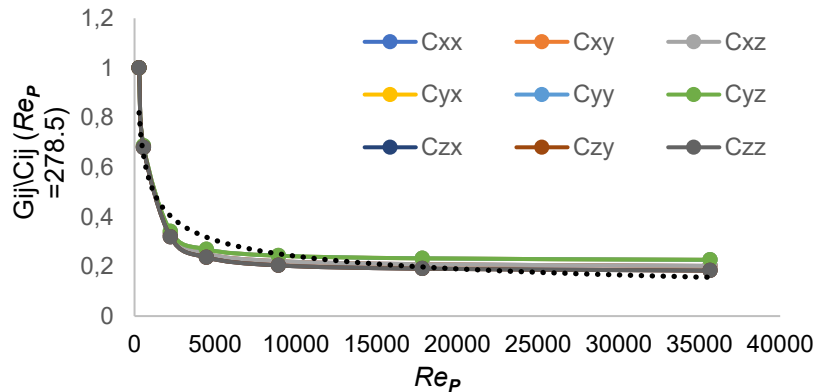


Figure 9. Normalized inertial resistance tensor by lower velocity.

## 6. Conclusion

The impact of particles' orientation on the pressure drop over a packed bed of ellipsoidal particles was investigated using the DEM/CFD approach, and the output results were validated with an experimental model. Moreover, pressure drop using a porous media approach was investigated and an equation was derived with the inertial tensor of particle Reynolds number dependence. Both results were validated with experimental output for a packed bed of crushed rocks. The models' findings underestimated the crushed rocks by less than 20% for horizontal and vertical flow, except for the DEM/CFD model, which over predicted the crushed rocks by 40% in vertical flow. This underprediction may be due to the fact that the DEM/CFD models shrank by 2.25%.

## Data availability statement

Project data will be available on SunScholar upon graduation.

## Author contributions

Author: Elzubeir Badawi Elzubeir Hassan; Designed the study, conducted the literature review, built the simulation and the practical models, collected and analyzed the data, and wrote the manuscript.

Author: Jaap Hoffmann; Supervised the research study.

All authors reviewed and agreed on the final version of the paper.

## Competing interests

The authors declare that they have no competing interests.



## Acknowledgement

The authors acknowledge the Solar Thermal Energy Group (STERG) and Stellenbosch University department of M&M for their funding and the Centre for High Performance Computing (CHPC) for providing computational resources for this research.

## References

1. K.G. Allen. "Rock bed thermal storage for concentrating solar power plants." PhD diss., Stellenbosch: Stellenbosch University, 2014.
2. R. K. Niven. "Physical insight into the Ergun and Wen & Yu equations for fluid flow in packed and fluidised beds." *Chemical Engineering Science* 57, no. 3 (2002): 527-534, [https://doi.org/10.1016/S0009-2509\(01\)00371-2](https://doi.org/10.1016/S0009-2509(01)00371-2).
3. E. Erdim, Ö. Akgiray, and I. Demir. "A revisit of pressure drop-flow rate correlations for packed beds of spheres." *Powder technology* 283 (2015): 488-504, <https://doi.org/10.1016/j.powtec.2015.06.017>.
4. K. Vollmari, T. Oschmann, S. Wirtz, and H. Kruggel-Emden. "Pressure drop investigations in packings of arbitrary shaped particles." *Powder Technology* 271 (2015): 109-124, <https://doi.org/10.1016/j.powtec.2014.11.001>.
5. K. G. Allen, T. W. Von Backström, and D. G. Kröger. "Packed Bed Pressure Drop Dependence on Particle Shape, Size Distribution, Packing Arrangement and Roughness." *Powder technology* 246 (2013): 590-600 <https://doi.org/10.1016/j.powtec.2013.06.022>.
6. S. Ergun. "Fluid flow through packed columns." *Chem. Eng. Prog.* 48 (1952): 89-94.
7. Du Plessis, J. Prieur, and Sonia Woudberg. "Pore-scale derivation of the Ergun equation to enhance its adaptability and generalization." *Chemical Engineering Science* 63, no. 9 (2008): 2576-2586, <https://doi.org/10.1016/j.ces.2008.02.017>.
8. R. E Hicks. "Pressure Drop in Packed Beds of Spheres." *Industrial & engineering chemistry fundamentals* 9, no. 3 (1970): 500-502, <https://doi.org/10.1021/i160035a032>.
9. D. P Jones. and Herman Krier. "Gas Flow Resistance Measurements Through Packed Beds at High Reynolds Numbers." (1983): 168-172, <https://doi.org/10.1115/1.3240959>.
10. R. Singh, R. P. Saini, and J. S. Saini, "Nusselt Number and Friction Factor Correlations for Packed Bed Solar Energy Storage System Having Large Sized elements of different shapes," *Sol. Energy*, vol. 80, no. 7, pp. 760–771, 2006, <https://doi.org/10.1016/j.solener.2005.07.001>.
11. A. D. R. Louw, "Discrete and Porous Computational Fluid Dynamics Modelling of an Air-Rock Bed Thermal Energy Storage System," M.Eng. Thesis, Stellenbosch University, 2014.
12. J. Hoffmann, "A CFD/DEM Approach to Determine the Flow Resistance of Randomly Packed Bed of Crushed Rock Particles," *Proc. 8th Int. Conf. Fluid Flow, Heat Mass Transf.*, no. 140, pp. 1–8, 2021,
13. J.E. Hoffmann and P.J. Lindeque. "Pressure drop through randomly packed beds of ellipsoidal particles." *Proceedings of HEFAT 2019* (2019), vol. 1, p. 6.
14. MC. Potgieter, CG. C.G., and JH. Kruger, "A 3D CFD model of the Flow and Heat Transfer Inside an Unstructured Bed Uniform Spheres," in *SACAM 2016*, 2016.
15. C. J. Coetzee and R. G. Nel. "Calibration of discrete element properties and the modelling of packed rock beds." *Powder technology* 264 (2014): 332-342 <https://doi.org/10.1016/j.powtec.2014.05.063>.
16. K.G. Allen, T.W. von Backstrom, and D.G Kroger "Rock bed pressure drop and heat transfer: Simple design correlations," *Solar Energy*, vol. 115, pp. 525–536, 2015.
17. B. Einfeld and K. Schnitzlein. "The influence of confining walls on the pressure drop in packed beds." *Chemical engineering science* 56, no. 14 (2001): 4321-4329, [https://doi.org/10.1016/S0009-2509\(00\)00533-9](https://doi.org/10.1016/S0009-2509(00)00533-9).

18. H. Blasius. "Das aehnlichkeitsgesetz bei reibungsvorgängen in flüssigkeiten." In Mitteilungen über Forschungsarbeiten auf dem Gebiete des Ingenieurwesens, pp. 1-41. Springer, Berlin, Heidelberg, 1913 [https://doi.org/10.1007/978-3-662-02239-9\\_1](https://doi.org/10.1007/978-3-662-02239-9_1).
19. J. Hoffmann, T. Manatsa, and J. Houtappels. "Flow Resistance of Randomly Packed Beds of Crushed Rock and Ellipsoidal Particles using CFD." Journal of Fluid Flow 9 (2022), <https://doi.org/10.11159/jffhmt.2022.002..>